

Novel testing equipment for fabric wrinkle resistance simulating actual wear

Chengxia Liu, Yaqin Fu and Niyang Wu

Textile Research Journal
2014, Vol. 84(10) 1059–1069
© The Author(s) 2014
Reprints and permissions:
sagepub.co.uk/journalsPermissions.nav
DOI: 10.1177/0040517513517963
trj.sagepub.com



Abstract

Wrinkling is one of the most important factors that determine the visual aesthetic of our clothes. To investigate wrinkling characteristics in actual wear and explore the relationship between the wrinkling caused by wearing and testing results of the wrinkle recovery angle (WRA) method, we made a device that can produce wrinkles very similar to those on clothes. Twenty-four fabrics were wrinkled by the device, and the images of wrinkled fabrics were analyzed. Wrinkle density (WD) was defined for wrinkling characterization. In addition, fractal dimension (FD) and gray level co-occurrence matrix (GLCM) variables were also used to describe wrinkling. These features were subsequently correlation analyzed with wrinkle recovery angles in 11 directions. The results show that both FD and WD can be used to characterize the wrinkling behavior and wrinkles generated by the device have obvious fractal characteristics. The larger the wrinkle recovery angle, the lower the fractal dimension. GLCM variables (energy, entropy, contrast, and correlation) had not shown obvious correlation with WRA. Furthermore, the wrinkling behavior in the 45° direction plays an important role in actual wear. It is advised that the WRA in the 45° direction be tested.

Keywords

fabric wrinkling, wrinkling analysis, wrinkle recovery angle, gray-level co-occurrence matrix, fractal dimension, actual wear

Wrinkling, caused by washing, drying, or wearing, is one of the most important characteristics in determining the visual aesthetic of clothes. The annoying wrinkles can not only decrease the quality of clothes but also affect the mood of the wearer. Therefore, it is of vital importance to precisely and objectively measure and evaluate the wrinkle resistance of fabrics. Conventionally, the American Association of Textile Chemists and Colorists (AATCC) TM 66-2008 and AATCC TM 128 2009 are the most commonly used testing methods. In the former method, wrinkles are caused by folding and compressing the fabric and the wrinkle recovery angle (WRA) of warp and weft directions is used to characterize the wrinkling behavior of the fabric. In the latter method, wrinkles are caused by rotating and compressing the fabric, and visual examination is used to evaluate the degree of wrinkling, during which wrinkle grades are acquired via experts by comparing the wrinkled fabrics with the standard replicas.

There are deficiencies in subjective evaluation such as inconsistency of the results, difficulty in

discriminating between the adjacent grades, and low efficiency. As a result, many experts have devoted themselves to more objective and reliable evaluation methods. In 1995, Youngjoo and Behnam analyzed the wrinkling degree of AATCC replica standards using a combination of texture and profile analysis techniques.¹ In 1999, Su and Xu used the laser line triangulation method to measure the three-dimensional (3D) surface data of a wrinkled fabric and built a neural network to perform wrinkle classification with regard to the visual standard.² In 2001, TJ Kang et al. measured the contour of the fabric surface with a stereo vision algorithm and subsequently used the data to evaluate fabric smoothness by fractal geometry.³ In 2003, Yang and

College of Materials and Textiles, Zhejiang Sci-Tech University, China

Corresponding author:

Yaqin Fu, College of Materials and Textiles, Zhejiang Sci-Tech University, Xiasha Higher Education District, Hangzhou, Zhejiang, 310018 China.
Email: fyq01@zstu.edu.cn

Huang at Dong Hua University reconstructed the 3D surface of an AATCC standard wrinkle pattern and measured its wrinkle degree using four index values that indicated the variation of the surface height.⁴

In recent years, other digital image processing technology and methods have been applied to develop a more automated and efficient fabric wrinkling evaluation system. In 2008, Behera and Mishra designed and built a system to measure the surface characteristics of a wrinkled fabric using image processing technology.⁵ Abril et al. proposed a method in which two images of the sample were obtained under orthogonal lateral illumination and a joint Canny edge detector was applied to integrate the wrinkling information of both images.⁶ In 2009, Yu and Yao presented a stereo vision system for reconstructing the 3D surface of a wrinkled fabric for detecting and characterizing wrinkles and evaluating the severity of wrinkling.⁷ In 2010, Zaouali et al. put forward an objective method enabling evaluation of multidirectional wrinkling of any colored fabric developed using digital image analysis.⁸ Hesarian studied the wrinkle properties of fabrics using the projected profile light line technique.⁹ In 2011, Sun et al. presented a novel wrinkle evaluation method that uses modified wavelet coefficients and optimized support vector machine (SVM) classifications to characterize and classify the wrinkling appearance of fabric.¹⁰ To evaluate the wrinkle grade of textile fabrics, Ravanidi and Pan established and examined the gray level co-occurrence matrix (GLCM) from an image of a wrinkled fabric surface in terms of the spatial displacement of its pixel pairs, number of gray levels, and angle orientations.¹¹

Summarizing the above methods and research, we know that there are still some problems in fabric wrinkle measurement and evaluation. In the AATCC TM 66-2008, it is possibly not sufficient or scientific to describe the comprehensive wrinkling behavior of a fabric only in terms of its wrinkle recovery angle in warp and weft directions because there is anisotropy in the wrinkle properties of fabrics.¹² Besides, warp and weft are not necessarily the directions that have closest relation to wrinkling degree in actual wear. With regard to the AATCC TM 128 2009, the wrinkles are similar to those in the process of washing and drying but they are quite different from those on wearing. In actual wear, wrinkles are caused by frequently bending and compressing, such as in the cases of the elbow and knee, while the fabric is twisted and compressed in the AATCC TM 128 2009.

Until now, studies on fabric wrinkling using computer vision technology have been mostly focused on wrinkles generated by the AATCC TM 128 2009. As has been analyzed above, there is considerable difference between wrinkles generated by the method that

might be classified as ‘wet wrinkles’ resulting from washing and drying and wrinkles caused by wearing that might be classified as ‘dry wrinkles’. Therefore, the existing research results are not necessarily suitable for wrinkling on clothes. To clarify the characteristics of wrinkles on clothes (dry wrinkles) and obtain the relationship between wrinkling on clothes and testing results of the AATCC TM 66-2008, we will explore a new wrinkle generating method in this study. Shinohara et al. studied the wrinkling characteristics when the fabric cylinder was compressed and established the mathematical models describing such wrinkles.^{13,14} To establish a convenient method characterizing fabric wrinkling during wear, a simple simulator was developed in our former study,¹⁵ in which the fabric cylinder was compressed. To improve the method further, in this paper, we present a fabric wrinkle generating device that simulates the bending movement of a human joint, and use image processing technology to analyze images of fabric wrinkled by this device. Finally, the wrinkling parameters will be extracted and compared with results of the AATCC TM 66-2008 technique.

Methods

Fabric wrinkle generating instrument

Garment wrinkling occurs most severely and commonly at the joints that bend and move frequently in daily life, such as the knee and elbow. Accordingly, we have designed a fabric wrinkle generating instrument that simulates the bending of the knee and elbow to produce wrinkling. As shown in Figure 1, the wrinkle generating instrument primarily consists of such materials as sponge stick①, in the center of which is flexible iron wire, cotton mass②, knitted fabric③, and fine iron wire. To make the device, several sponge sticks were bound together with

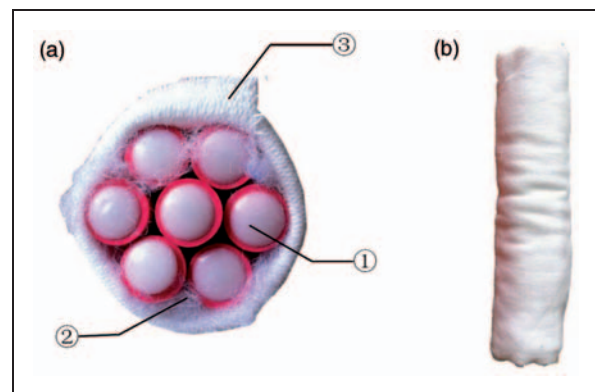


Figure 1. Fabric wrinkle generating device: (a) cross section structure of the instrument; (b) whole appearance of the device.

fine iron wire to simulate human joint bones and muscles. The outsides of the sponge sticks were padded with cotton, to simulate body fat, and elastic knitted fabric was wrapped outside the cotton, to simulate body skin (see Figure 1(a)). From Figure 1(b), it can be seen that the device looks like human arm to some extent. Hereafter, it is abbreviated as the ‘arm, which is 20 cm long and the girth being 16 cm.

Materials

Twenty-four fabrics with different fiber contents and weave structures were chosen to validate the wrinkle generating results of the instrument. All the fabrics were of solid color. The fabric parameters are shown in Table 1. Three swatches of 20 cm × 18 cm were ironed and cut for each fabric. Each swatch was folded in half face to face along the lengthwise grain, and sewn into a fabric cylinder with 0.5 cm seam allowance. Subsequently, the fabric cylinder was turned with right side out, being 17 cm girth and 20 cm length. Both

the sample preparation and the whole experiment were carried out in a standard atmosphere ($21 \pm 1^\circ\text{C}$, $65 \pm 2\%$ humidity).

Fabric wrinkle generating method

The sewn fabric cylinder was put on and wrapped over the ‘arm’ gently. The ‘arm’ was bent in half to form about 30° with the fabric seam opposite the bending direction. In Figure 2, two arms with fabric samples were put and positioned into the shorter end of a rectangular mouth of 15 cm × 9 cm to keep them bent and compressed with the same pressure and angle. Ten minutes later, the ‘arm’ was taken down. Then the fabric cylinder was taken off the ‘arm’ and spread gently, with the sewing thread removed as carefully as possible.

Comparison of the wrinkles

Wrinkles generated by the instrument and those on clothes are shown in Figure 3. Figure 3(a) and (b) are

Table 1. Parameters of fabrics studied

Fabric	Weave	Fiber content	Density (/10 cm)		Mass per unit area (g/m^2)	Thickness (mm)	Color
			warp	weft			
F1	plain	100% L	80	73	192	0.4	dark khaki
F2	plain	100% C	103	60	247	0.25	coral
F3	plain	100% S	169	136	195	0.23	black
F4	plain	55 S/45 P	65	71	226	0.19	cream
F5	plain	100% S	119	31	198	0.21	purple
F6	plain	100% S	129	72	150	0.35	brown
F7	plain	100% W	51	55	81	0.26	cyan
F8	plain	100% C	83	84	219	0.21	yellow
F9	twill	100% C	112	40	56	0.56	khaki
F10	plain	100% C	60	54	126	0.23	gray
F11	plain	100% C	106	57	97	0.27	blue
F12	satin	50 C/50 P	136	70	128	0.49	pink
F13	plain	100% L	48	38	146	0.42	light khaki
F14	plain	55 L/45 C	51	39	151	0.37	dark blue
F15	twill	85 W/15 P	60	49	209	0.38	orchid
F16	twill	100% W	42	35	188	0.62	olive drab
F17	twill	60 W/40 P	75	49	62	0.52	moss green
F18	twill	100% P	122	68	76	0.13	cream
F19	twill	100% P	85	45	207	0.32	red
F20	twill	100% P	160	69	113	0.13	blue
F21	plain	100% P	91	66	194	0.08	orange
F22	plain	100% V	455	250	119	0.22	black
F23	plain	100%V	150	108	380	0.67	navy blue
F24	plain	100% C	225	227	147	0.53	light green

C: cotton, L: linen, S: silk, W: wool, P: polyester, V: viscose

wrinkles produced by the instrument, in which Figure 3(a) shows wrinkles on the device and Figure 3(b) shows wrinkles when the fabric is taken off the device and spread. Figure 3(c) and (d) are photos taken from ordinary clothes in daily life, representing the most ordinary and typical wrinkles occurring in wear.¹⁵ By comparing Figure 3(a) and (c) with Figure 3(b) and (d), respectively, we observed that the wrinkles generated by the instrument and those on clothes by wear are extremely similar. Wrinkles generated by the instrument and by wearing are composed of lozenges whose centers sink and whose sides extrude, while after the fabric or clothes are taken off and spread, the wrinkling features change inversely. The wrinkles now are composed of lozenges with a protruding line along their main axis.

Image capture

After recovering from the wrinkling for 5 min, the wrinkled fabric was scanned with a LiDE210 CanoScan scanner to capture the image with a resolution of 300 dpi. When scanning, something small



Figure 2. Bending and compressing the fabric cylinder.

was put between the wrinkled fabric and the cover of the scanner to give enough space for the wrinkle, avoiding pressure from the cover. After capture, the image was cut into 256 pixel \times 256 pixel tiles for further processing and analysis.

Wrinkle characterization

The images were processed by software developed in MATLAB, widely applied for image processing. Wrinkling was characterized with three types of parameters, i.e. wrinkle density, fractal dimension, and GLCM variables.

Wrinkle density (WD)

As shown in Figure 4, the scanned color image was converted into a gray-level image.⁸ To improve the perception and contours of the wrinkles, the gray-level images were enhanced. To reduce the noise of the image, the enhanced image was median filtered. The filtered image was converted to a binary image, which was subsequently edge detected to obtain wrinkling lines.

The white lines in Figure 4(f) represent wrinkling lines on the fabric. The number of white lines could indicate the severity of wrinkling. Therefore, wrinkle density (WD) was defined as the percentage of white pixels to the total number of pixels in the edge detected image, which was calculated according to:

$$WD = \frac{w_n}{A} \times 100\% \quad (1)$$

where w_n is number of white pixels and A is the total number of pixels ($256 \times 256 = 65,536$).

Fractal dimension (FD)

Fractal theory is called geometry of nature and can be defined as images that have self-similarity to some

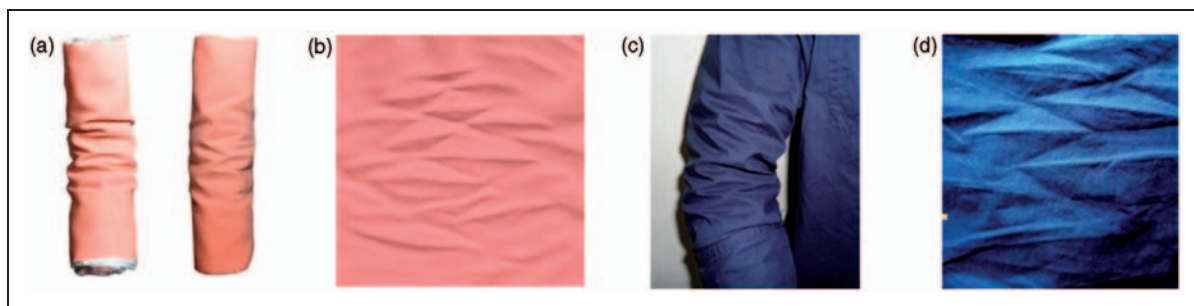


Figure 3. Wrinkles generated by the device and those on clothes: (a) wrinkles on the device; (b) wrinkles when the fabric is taken off the device and spread; (c) wrinkles on clothes; (d) wrinkles when clothes are spread.

extent, and whose complexity can be expressed by fractal dimensions.¹⁶ To test and verify whether the wrinkle generated by the instrument has fractal features, box-counting dimension was chosen to calculate the fractal dimension. In the calculation of box dimension, the image is first segmented into grids with side length δ , and the number of grids N needed to cover the required area in the image is then calculated. If the image has fractal features, when δ is approximated to 0, the FD can be solved. So for the decreasing sequence of numbers δ , we can practice linear-regression analysis of $\log 1/\delta$ and $\log N$ in double logarithmic coordinate system. If there is a linear relationship, then the slope will be the approximated value of the FD, which can be calculated according to:

$$FD = \lim_{\delta \rightarrow 0} \frac{\log N}{\log 1/\delta} \quad (2)$$

where N is the number of grids that could cover the required area in the image and δ is the side length of grids.

Gray level co-occurrence matrix (GLCM) variables

The GLCM is widely used in texture description by characterizing the spatial distributions of gray levels in the image.^{17,18} GLCM is defined as the probability $p(i, j)$ of a pixel of gray level i occurring in the specified spatial relationship of (d, θ) with a gray level j , in which

d and θ are the distance and positional angle between the two gray-level pairs (i, j) .¹¹ Conventionally, the positional angles consist of 0° , 45° , 90° , and 135° . In this work, the images were monochromatic with 16 gray levels, d was 1, and the variables were as listed below.

Energy or angular second moment measures the textural homogeneity. The larger the energy, the higher is the textural homogeneity. It is calculated according to:

$$Energy = \sum_i \sum_j \{p(i, j)\}^2 \quad (3)$$

where $p(i, j)$ is the probability of a pixel of gray level i occurring in the specified spatial relationship with a gray level j , $i, j=0, 1, \dots, N-1$, where N is the number of gray levels in the image.

Entropy, which indicates the disorder of the texture, is calculated according to:

$$Entropy = - \sum_i \sum_j p(i, j) \log\{p(i, j)\} \quad (4)$$

where $p(i, j)$ has the same meaning as that in equation (3).

Correlation, which represents the linear dependence between gray levels in the texture, is calculated according to:

$$Correlation = \frac{\sum_i \sum_j (ij) p(i, j) - \mu_x \mu_y}{\delta_x \delta_y} \quad (5)$$

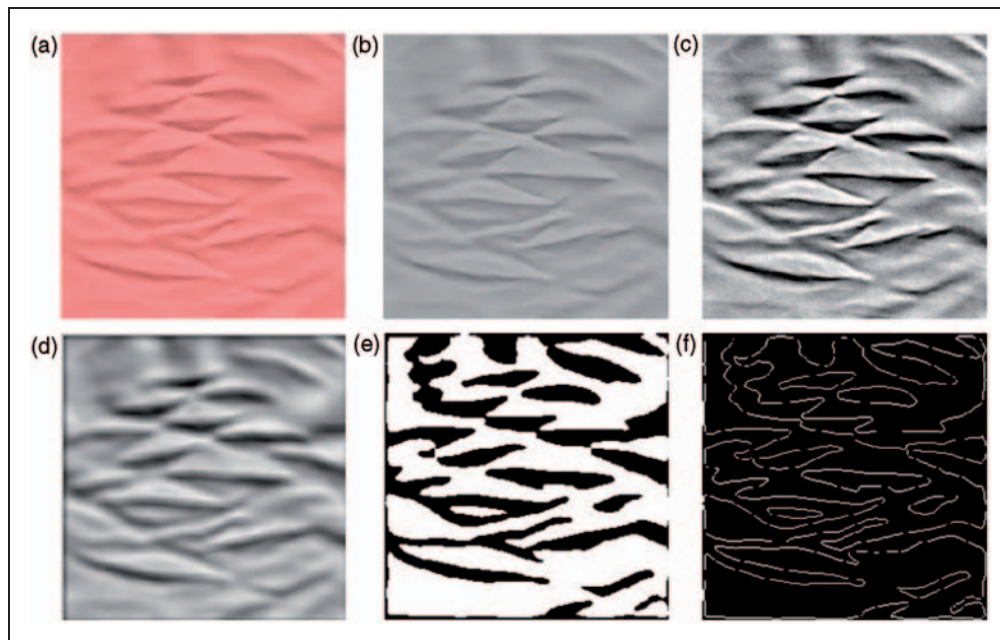


Figure 4. The image processing: (a) color image; (b) gray-level image; (c) enhanced image; (d) noise-reduced image; (e) binary image; (f) edge-detected image.

where $\mu_x = \sum_i i \sum_j p(i,j)$, $\mu_y = \sum_j j \sum_i p(i,j)$, and $\delta_x^2 = \sum_i (i - \mu_x)^2 \sum_j p(i,j)$, $\delta_y^2 = \sum_j (j - \mu_y)^2 \sum_i p(i,j)$.

Contrast, which reflects the local variations of texture, is calculated according to:

$$\text{Contrast} = \sum_i \sum_j (i - j)^2 p(i,j) \quad (6)$$

where $p(i, j)$ has the same meaning as that in equation (3).

Wrinkle recovery angle (WRA)

Creasing in the traditional AATCC TM 66-2008 test is not sufficiently realistically described, because the specimen of fabric is creased only in two directions (warp and weft), which does not correspond with the real creasing of the worn fabric.¹⁹ To measure the wrinkling behavior of fabrics in different directions, wrinkle recovery angles (WRAs) in every 10° direction from 0° (weft) to 90° (warp) were tested, rather than only

warp and weft as required in AATCC TM 66-2008. In addition, WRA in the 45° direction was also considered. The WRA in every direction was taken as the average of three measurements.

Results and discussion

To explore characteristics of wrinkles produced by the novel device, image processing, the fractal method, and GLCM were applied to analyze the wrinkled image. After that, AATCC TM 66-2008 was conducted, and the WRA of 24 fabrics in 11 directions was measured. Test results for WRA are shown in Table 2. From the test results, it can be seen that there is a significant difference between wrinkling performance in different directions.

Relationship between WD and WRA in different directions

The new parameter of wrinkle density (WD) is shown in Table 3. To investigate the relationship between the

Table 2. Wrinkle recovery angle in different directions (expressed in degrees)

Fabric	0°	10°	20°	30°	40°	45°	50°	60°	70°	80°	90°
F1	84.33	85.33	88.67	82.67	81.00	85.00	90.67	78.33	70.67	69.33	79.67
F2	88.00	86.33	111.33	90.00	90.33	94.00	98.67	95.33	92.33	94.67	103.00
F3	39.00	39.33	63.33	50.00	63.33	69.00	70.33	61.33	68.67	59.67	64.00
F4	137.00	153.00	145.33	148.67	143.33	149.67	152.00	146.33	145.67	156.67	148.00
F5	99.00	114.67	122.33	127.00	121.20	137.00	125.33	130.33	130.33	128.00	124.00
F6	135.00	141.33	143.00	137.33	144.00	142.67	148.00	137.67	144.67	145.67	141.00
F7	80.00	95.33	99.67	95.67	112.33	96.00	102.00	96.00	96.33	98.00	89.00
F8	94.33	102.00	117.67	110.33	91.25	85.00	95.33	94.67	83.67	94.33	64.00
F9	76.00	65.00	125.67	100.67	105.67	110.00	120.00	108.67	106.50	84.33	85.67
F10	112.00	105.33	124.33	112.33	90.67	96.33	116.25	99.67	84.67	87.00	89.00
F11	147.00	132.67	131.00	130.00	125.67	120.00	111.33	108.00	115.33	119.33	129.00
F12	115.00	120.00	135.00	132.33	125.00	108.00	130.00	127.00	114.00	111.33	115.33
F13	124.67	141.00	141.67	140.00	136.67	145.00	145.33	129.67	130.33	134.67	126.33
F14	142.67	156.33	147.33	159.33	150.33	155.00	153.67	151.67	144.33	149.67	145.33
F15	155.67	143.67	155.33	144.00	157.00	151.00	150.33	145.67	142.00	154.33	153.00
F16	146.00	139.33	143.00	144.50	145.00	138.00	143.33	144.00	138.33	144.33	140.00
F17	157.33	140.33	155.50	152.00	154.33	150.00	154.67	146.00	147.33	149.33	154.33
F18	115.50	103.33	135.33	124.00	138.67	148.67	143.33	144.33	139.33	137.50	140.00
F19	131.67	145.67	155.00	145.33	146.33	148.00	145.67	148.67	130.33	134.83	135.00
F20	120.17	149.00	147.00	150.67	155.00	159.00	160.00	153.00	155.00	133.50	146.67
F21	117.83	148.00	145.00	149.00	154.00	154.67	150.33	147.00	148.67	132.00	144.00
F22	63.30	67.33	100.67	90.00	92.67	100.00	101.33	92.33	87.67	91.00	76.33
F23	67.67	62.00	94.00	83.67	95.67	83.67	94.33	77.00	83.67	76.67	77.67
F24	65.33	63.33	76.00	60.33	58.00	65.17	68.33	61.33	58.67	60.33	59.67

Values represent the average of three data points.

WD in the new device and the WRA in different directions, correlation analysis was used.

Figure 5 shows a line chart of Pearson's correlation coefficient between WD and WRA in different directions. A line chart is an effective descriptive tool to indicate the distribution of a data set. In the plot, all the Pearson's correlation values are highly significant at

0.01 level (bilateral). From Figure 5, it is clear that WD acquired by the image processing has negative correlation with WRAs in different directions. Nevertheless, the WRA in different directions has a different correlation coefficient value with WD. The WRA in the 45° (true bias) direction has the highest correlation coefficient value with WD, and the value in 0° (weft) direction has the lowest. From 0° to 45°, the correlation coefficient value increases gradually, while from 45° to 90° (warp), the value decreases somewhat.

Next, linear regression was carried out to obtain the exact equation between the two groups of wrinkling parameters. Table 4 shows the regression results. From Table 4, it can be seen that in the first regression method (stepwise), only WRA₄₅ (WRA in 45° direction) entered the equation. The Sig (level of significance) is $F < 0.001$, which indicates that equation (7) is adequate to the obtained results at a significance level 0.05. While in the second regression method (Enter), in which all the WRAs are entered, the equation is not satisfied.

Table 3. Calculated wrinkle density (WD) (expressed in %)

Fabric	WD	Fabric	WD	Fabric	WD	Fabric	WD
F1	7.67	F7	7.71	F13	5.25	F19	5.45
F2	7.44	F8	6.64	F14	5.81	F20	5.05
F3	7.50	F9	7.42	F15	5.04	F21	5.27
F4	4.51	F10	7.68	F16	5.97	F22	7.68
F5	6.76	F11	7.27	F17	3.69	F23	6.82
F6	7.36	F12	6.79	F18	5.62	F24	6.49

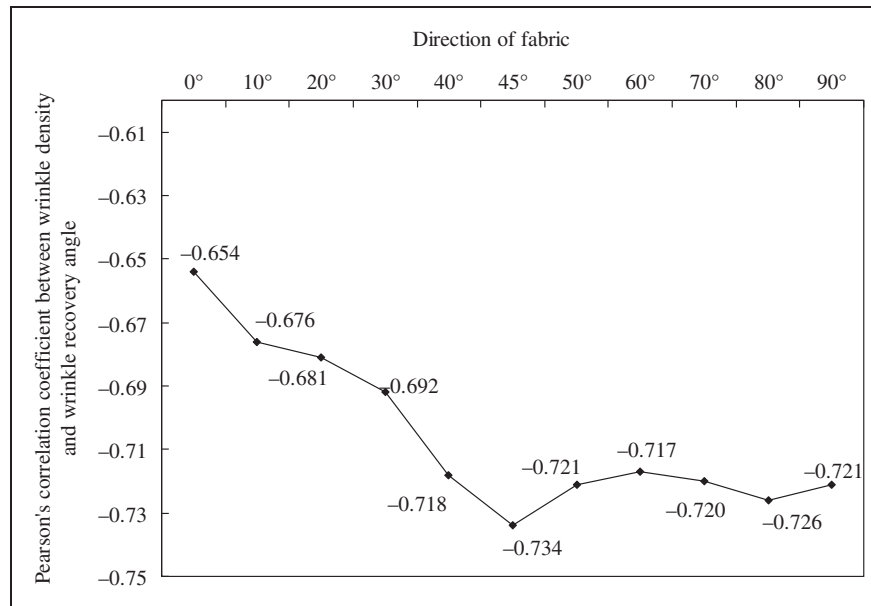


Figure 5. Pearson's correlation coefficient between wrinkle density and wrinkle recovery angles in different directions of all the fabrics.

Table 4. Linear regression of wrinkle density (WD) and wrinkle recovery angle (WRA)

Method	Variable entered	Modal R ²	Anova		Equation
			F	Sig	
Stepwise	WRA ₄₅	0.538	25.662	< 0.001	WD = 9.716 - 0.028WRA ₄₅ (7)
Enter	Eleven WRAs	0.557	1.372	0.297 (>0.05)	WD = 9.735 - 0.006WRA ₀ - 0.003WRA ₁₀ + 0.006WRA ₂₀ + 0.012WRA ₃₀ - 0.003WRA ₄₀ - 0.02WRA ₄₅ - 0.018WRA ₅₀ + 0.003WRA ₆₀ + 0.10WRA ₇₀ - 0.11WRA ₈₀ + 0.02WRA ₉₀ (8)

Relationship between FD and WRA in different directions

As has been stated before, the value of fractal dimension (FD) can be calculated by practicing linear-regression analysis of $\log 1/\delta$ and $\log N$ in a double logarithmic coordinate system. Taking F7 fabric as an example, the curve between $\log N$ and $\log 1/\delta$ of F7 is shown in Figure 6.

From Figure 6, we can clearly see that there is a good linearly dependent line between $\log N$ and $\log 1/\delta$, so the gradient of the line can be used to calculate the value of FD. In the case of F7 fabric, the FD is 1.97. It is found that similar lines have been obtained with other fabrics, which proves that the wrinkle generated by the device has obvious fractal features. All the calculated FD values of the 24 fabrics are shown in Table 5.

Figure 7 shows the line chart of Pearson's correlation coefficient between FD and WRA in different directions for the 24 fabrics. In the plot, all the Pearson's correlation values are highly significant at 0.01 level (bilateral). From Figure 7, it can be seen that the FD also has negative correlation with the WRAs in different directions. That is, the larger the WRA, the lower is the FD. In other words, the FD can serve as a measure of the roughness or wrinkling degree of fabrics. Furthermore, Figure 7 displays a similar change trend to Figure 5, in that the Pearson's correlation coefficient of 0° is the lowest, then increases until 45° and decreases somewhat after that.

Table 6 shows the regression results of FD and WRA. From Table 6, it can be seen that in the first regression method (stepwise), only WRA_{45} entered the equation, in which the Sig is $F < 0.001$. In the second

regression method (Enter), when all the WRA are entered, the equation is also satisfied (the Sig is $F < 0.05$). This indicates that both equations (9) and (10) are adequate for the obtained results at a

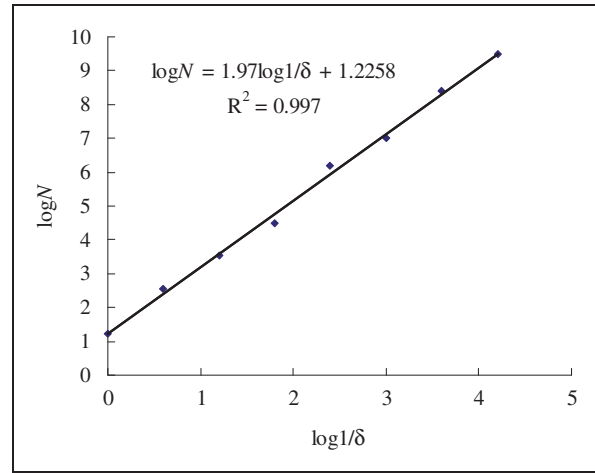


Figure 6. The curve between $\log N$ and $\log 1/\delta$ of F7 fabric.

Table 5. Calculated fractal dimension (FD) values

F	FD	F	FD	F	FD	F	FD
F1	1.94	F7	1.97	F13	1.84	F19	1.83
F2	1.95	F8	1.93	F14	1.79	F20	1.81
F3	1.96	F9	1.94	F15	1.81	F21	1.86
F4	1.88	F10	1.95	F16	1.86	F22	1.88
F5	1.88	F11	1.91	F17	1.75	F23	1.92
F6	1.83	F12	1.88	F18	1.89	F24	1.93

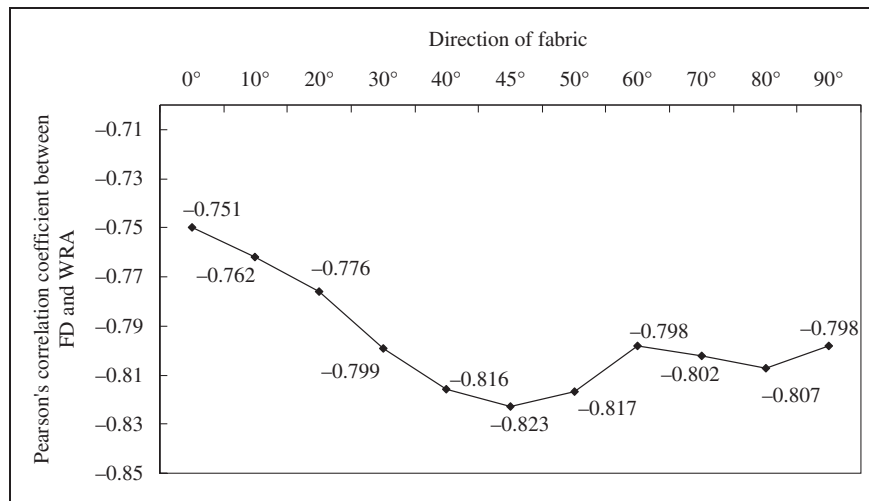


Figure 7. Pearson's correlation coefficients between fractal dimension (FD) and wrinkle recovery angle (WRA) in different directions of all the fabrics.

Table 6. Results of linear regression of fractal dimension (FD) and wrinkling recovery angle (WRA)

Method	Variable entered	Modal R^2	Anova		Equation
			F	Sig	
Stepwise	WRA ₄₅	0.677	46.010	<0.001	FD = 2.074 - 0.002WRA ₄₅ (9)
Enter	Eleven WRAs	0.721	2.819	0.044 (<0.05)	FD = 2.072 - 0.0007WRA ₀ - 0.0006WRA ₁₀ + 0.001WRA ₂₀ + 0.001WRA ₃₀ - 0.001WRA ₄₀ - 0.0005WRA ₄₅ - 0.01WRA ₅₀ + 0.001WRA ₆₀ + 0.001WRA ₇₀ - 0.0005WRA ₈₀ + 0.0003WRA ₉₀ (10)

Table 7. Calculated gray level co-occurrence matrix (GLCM) variables

F	Energy	Entropy	Contrast	Correlation	F	Energy	Entropy	Contrast	Correlation
F1	0.92	1.92	1.31	5.24	F13	2.38	1.00	0.49	10.45
F2	0.91	2.07	1.18	3.50	F14	3.29	0.45	0.22	35.98
F3	2.50	0.87	0.35	17.86	F15	1.56	1.17	0.63	10.99
F4	1.52	1.16	0.54	11.28	F16	1.30	1.52	1.05	7.32
F5	1.02	1.78	1.21	5.82	F17	0.64	2.10	3.34	1.26
F6	2.14	1.03	0.96	7.12	F18	0.94	1.98	0.80	3.56
F7	1.19	1.68	0.74	6.14	F19	0.64	2.10	3.34	1.26
F8	0.78	2.10	0.93	3.48	F20	1.12	1.70	1.00	5.94
F9	1.11	1.88	0.95	4.74	F21	0.94	1.69	0.55	4.56
F10	0.77	2.13	1.34	3.91	F22	1.09	2.00	1.32	3.65
F11	1.14	1.69	0.69	5.77	F23	1.85	1.04	0.64	11.95
F12	0.65	2.28	1.10	2.83	F24	0.99	1.89	0.89	4.34

significance level 0.05. Comparing R^2 values of equations (9) and (10) and equation (7), we find that R^2 of equation (10) is the highest (0.721), R^2 of equation (9) is the middle value (0.677), and that of equation (7) is the lowest (0.538). It is shown that the fitting effect of equation (10) is the best. In the same stepwise regression method, the fitting effect of equation (9) is better than that of equation (7). It seems that FD is more appropriate to be used to characterize the wrinkling degree than WD and WRA₄₅ has more significant correlation with wrinkling behavior in the new method than WRA in other directions.

Relationship between GLCM and WRA in different directions

Table 7 shows GLCM variables (the total energy, entropy, contrast, and correlation) of four angles (0°, 45°, 90°, and 135°). Figure 8 shows the scatter diagram of WRA in the 45° direction and the GLCM variables. From Figure 8, it can be seen that there is no obvious correlation between GLCM variables and WRA in the 45° direction. WRA in other directions does not show obvious linear correlation with GLCM variables.

To sum up, it has been shown from two parameters of wrinkling characterization (WD and FD) that wrinkling behavior in the 45° direction plays an important role in how clothes will resist creasing. Besides, from the Pearson's correlation coefficient, we know that wrinkle resistance in the warp direction has significantly higher correlation than weft direction with the wrinkling test results obtained by our new method, which is in fact a simulation of actual wear. In fashion design, the warp direction of the fabric is always used as lengthwise grain of clothes, and when human joints bend and move the warp yarn of clothes will be folded and compressed, just as happens in the WRA measurement of the warp direction. This explains why the WRA in the warp (90°) direction contributes more than that in the weft (0°) direction to wrinkling behavior in actual wear. As for the bias direction, Figure 3 shows the wrinkling line on clothes consists of two groups, those close to the horizontal direction and those in a slanting direction whose number exceeds that of the horizontal ones. The large number of slanting wrinkling lines can be an explanation of why Pearson's correlation coefficient value of the wrinkle recovery angle in the 45° direction is relatively high with respect to wrinkling behavior in

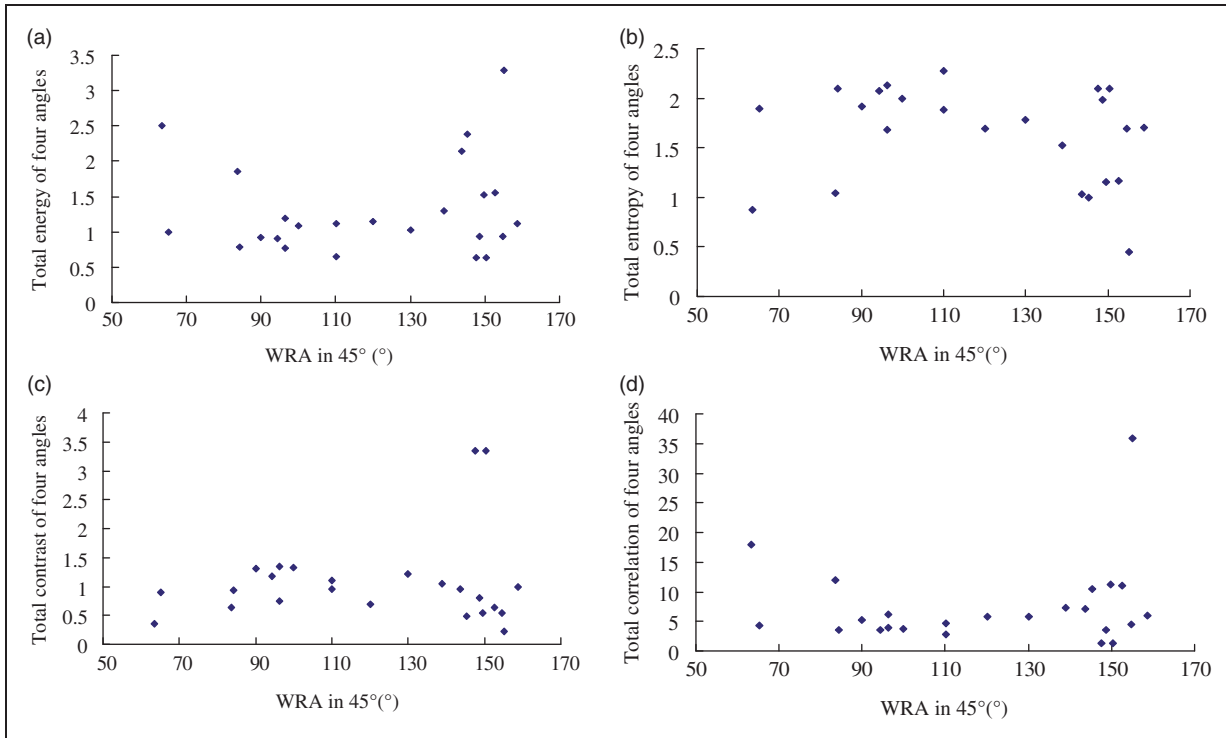


Figure 8. Pearson's correlation coefficients between fractal dimension (FD) and wrinling recovery angle (WRA) in different directions.

actual wear. Consequently, it is advised that WRA in the 45° direction be tested, rather than only warp and weft directions as required in the AATCC TM 66-2008 test.

Conclusions

The device presented in this paper can generate wrinkles very similar to those caused by wearing, which take the shape of a diamond with four slanting sides and an almost horizontal line. Wrinkles generated by the device have obvious fractal features, and with increasing wrinkle recovery angle (WRA), the fractal dimension (FD) decreases. Both FD and wrinkling density (WD) can be used to characterize the wrinkling behavior. However, the GLCM variables (energy, entropy, contrast, and correlation) have not shown obvious correlation with WRA. Moreover, wrinkling behavior in the 45° direction plays an important part in the crease resistance of actual wear. It is advisable that WRA in the 45° direction be measured in the AATCC TM 66-2008 test.

The equation, $WD = 9.716 - 0.028WRA_{45}$, can be used to predict the WD of wrinkled fabric in actual wear. The FD of wrinkled fabric in actual wear could be predicted by the two equations as $FD = 2.074 - 0.002WRA_{45}$ or $FD = 2.072 - 0.0007WRA_0 - 0.0006WRA_{10} + 0.001WRA_{20} +$

$0.001WRA_{30} - 0.001WRA_{40} - 0.0005WRA_{45} - 0.01WRA_{50} + 0.001WRA_{60} + 0.001WRA_{70} - 0.0005WRA_{80} + 0.0003WRA_{90}$.

It is simple and convenient to estimate the wrinkling characteristic of fabric during actual wear with WRA in the 45° direction.

Funding

This work was supported by the Natural Science Foundation of Zhejiang Province (grant number LQ13E050017), the Open Fund of Zhejiang Provincial Colleges and Universities Priority Subject in Key Disciplines (grant number 2013KF07), and the Open Fund of Zhejiang Provincial Research Centre of Clothing Engineering Technology (grant number 2012007).

References

1. Youngjoo N and Behnam P. Assessing wrinkling using image analysis and replicate standards. *Text Res J* 1995; 65: 149–157.
2. Su J and Xu B. Fabric wrinkle evaluation using laser triangulation and neural network classifier. *Opt Eng* 1999; 38: 1688–1693.
3. Kang TJ, Cho DH and Kim SM. New objective evaluation of fabric smoothness appearance. *Text Res J* 2001; 71: 446–453.
4. Yang XB and Huang XB. Evaluating fabric wrinkle degree with a photometric stereo method. *Text Res J* 2003; 73: 451–454.

5. Behera BK and Mishra R. Measurement of fabric wrinkle using digital image processing. *Indian J Fiber Text* 2008; 33: 30–36.
6. Abril HC, Millan MS and Valencia E. Influence of the wrinkle perception with distance in the objective evaluation of fabric smoothness. *J Opt A Pure Appl Opt* 2008; 10: 1–10.
7. Yu W and Yao M. 3-D surface reconstruction and evaluation of wrinkled fabrics by stereo vision. *Text Res J* 2009; 79: 36–46.
8. Zaouali R, Msahli S and Sakli F. Fabric wrinkling evaluation: a method developed using digital image analysis. *J Text Inst* 2010; 101: 1057–1067.
9. Hesarian MS. Evaluation of fabric wrinkle by projected profile light line method. *J Text Inst* 2010; 101: 463–470.
10. Sun JJ, Yao M, Xu B, et al. Fabric wrinkle characterization and classification using modified wavelet coefficients and support-vector-machine classifiers. *Text Res J* 2011; 81: 902–913.
11. Ravanidi SAH and Pan N. The influence of gray-level co-occurrence matrix variables on the textural features of wrinkled fabric surfaces. *J Text Inst* 2011; 102: 315–321.
12. Merati A and Patir H. Anisotropy in wrinkle properties of woven fabric. *J Text Inst* 2011; 102: 639–646.
13. Shinohara A, Ni QQ and Takatera M. Geometry and mechanics of the buckling wrinkle in fabrics. Part I: Characteristics of the buckling wrinkle. *Text Res J* 1991; 61: 94–100.
14. Shinohara A, Ni QQ and Takatera M. Geometry and mechanics of the buckling wrinkle in fabrics. Part II: Buckling model of a woven fabric cylinder in axial compression. *Text Res J* 1991; 61: 100–105.
15. Liu CC. New method of fabric wrinkle measurement based on image processing. *Fibres Text East Eur* 2014; 103: 51–55.
16. Mandelbrot BB. *The fractal geometry of nature*. New York: WH Freeman & Company, 1983, pp.14–43.
17. Lin JJ. Applying a co-occurrence matrix to automatic inspection of weaving density for woven fabrics. *Text Res J* 2002; 72: 486–490.
18. Tolba AS, Khan HA, Mutawa AM, et al. Decision fusion for visual inspection of textiles. *Text Res J* 2010; 80: 2094–2106.
19. Fridrichova L and Zelova K. Objective evaluation of multidirectional fabric creasing. *J Text Inst* 2011; 102: 719–725.